PHYSICAL REVIEW C **81**, 011602(R) (2010)

# Benchmarking a surrogate reaction for neutron capture

R. Hatarik,[1,*] L. A. Bernstein,[2] J. A. Cizewski,[1] D. L. Bleuel,[2] J. T. Harke,[2] J. E. Escher,[2] J. Gibelin,[3] B. L. Goldblum,[3,4] A. M. Hatarik,[1] S. R. Lesher,[2] P. D. O'Malley,[1] L. Phair,[3] E. Rodriguez-Vieitez,[3] T. Swan,[1,5] and M. Wiedeking[2,3]

[1]*Rutgers University, New Brunswick, New Jersey 08903, USA*

[2]*Lawrence Livermore National Laboratory, Livermore, California 94550, USA*

[3]*Lawrence Berkeley National Laboratory, Berkeley, California 94720, USA*

[4]*Nuclear Engineering Department, University of California, Berkeley, California 94720, USA*

[5]*University of Surrey, Guildford GU2 7XH, Surrey, United Kingdom*

(Received 11 December 2009; published 19 January 2010)

$^{171,173}$Yb$(d,p\gamma)$ reactions are measured, with the goal of extracting the neutron capture cross-section ratio as a function of the neutron energy using the external surrogate ratio method. The cross-section ratios obtained are compared to the known neutron capture cross sections. Although the Weisskopf-Ewing limit is demonstrated not to apply for these low neutron energies, a prescription for deducing surrogate cross sections is presented. The surrogate cross-section ratios deduced from the $^{171,173}$Yb$(d,p\gamma)$ measurements agree with the neutron capture results within 15%.

DOI: 10.1103/PhysRevC.81.011602 PACS number(s): 24.87.+y, 25.40.Lw, 25.60.Je, 27.70.+q

Most of the heavy elements ($A > 60$) in the universe have been created via neutron capture by either the *s* or the *r* process. At present-day facilities many *s*-process branch points cannot be measured directly with radioactive targets and neutron beams, because the target decay background by far outweighs the $\gamma$ emission of the neutron capture reaction. Neutron capture cross sections on heavy nuclei can also affect the synthesis of nuclei in the *r* process, in particular during freeze-out. For example, recent studies [1,2] have shown significant (>10%) changes in *r*-process abundances because of uncertainties in $(n,\gamma)$ rates on nuclei near $^{132}$Sn. Neutron capture cross sections on unstable nuclei are also needed for stockpile stewardship science [3] and performance calculations for advanced nuclear power reactors [4]. This work investigated the extent to which the $(d,p\gamma)$ transfer reaction could be used as a surrogate reaction for neutron capture.

Statistical Hauser-Feshbach [5] calculations have been employed to model compound-nuclear-reaction cross sections for neutron-induced reactions on many isotopes. Because the accuracy of the predicted cross sections is known to be limited in situations where little experimental information is available to constrain the description of the decay of the compound nucleus, there is significant interest in exploring indirect methods to provide the cross section of interest. Starting with the pioneering work of Cramer and Britt [6], surrogates for neutron-induced reactions, in which compound nuclei are populated in a light-ion-induced reaction, have been developed to provide information on neutron-induced-reaction cross sections. Surrogate methods have been extensively applied for $(n,f)$ reactions [7–12]. Because of the importance of $(n,\gamma)$-reaction cross sections it is critical to identify a valid surrogate for this reaction, if possible. Recently $(^3$He,p$\gamma)$ was used as a surrogate for $(n,\gamma)$ [13], in which deduced surrogate cross sections were compared to databases and predictions as opposed to experimental data. Therefore it is difficult to validate the deduced $(n,\gamma)$ cross sections, especially given the need to subtract contributions from surrogate $(n,n')$ reactions with measurements with very low-resolution $C_6D_6$ detectors. In another recent work the $(^3$He,$^3$He$'\gamma)$ and $(^3$He,$\alpha\gamma)$ reactions [14] were used to obtain a surrogate cross-section ratio for $^{170}$Yb and $^{160}$Dy. In that work NaI detectors were used to gate on the statistical $\gamma$ cascade and the result was in agreement with measured $(n,\gamma)$ cross sections. Concurrent with the present work, the $(d,p)$ reaction was used to deduce the $^{235}$U$(n,\gamma)$ cross sections relative to $^{235}$U$(n,f)$ and compared to ENDF evaluations [15].

The $(d,p\gamma)$ reaction at moderate beam energies (10–20 MeV) brings in a relatively low angular momentum, similar to $(n,\gamma)$, which is most often dominated by *s*-wave capture at neutron energies important for astrophysics and most applications. The $(d,p\gamma)$ reaction has also been demonstrated in inverse kinematics [16], when a beam of the heavy incident particle interacts with a $CD_2$ target and reaction protons are measured in coincidence with $\gamma$ rays. Such inverse kinematics, with rare isotope beams, is the only way to measure a surrogate reaction with a compound nucleus that cannot be produced from a reaction involving only stable nuclei. The kinematics of these inverse reactions is such that $(d,p)$-reaction protons (at forward angles in the center of mass) are preferentially detected at back angles in the laboratory. Alternative surrogate reactions, such as inelastic scattering $(p,p')$ with $CH_2$ targets, would have light reaction products at forward angles, competing with elastic scattering from the target, as well as protons from other reactions, such as fusion of the heavy beam with the carbon in the target.

Given the importance of $(n,\gamma)$ reactions for basic and applied nuclear physics as well as astrophysics and the possibility of using $(d,p\gamma)$ as a surrogate for neutron capture with rare isotope beams, we performed the present work as a benchmark test to validate whether $(d,p\gamma)$ can be used as a surrogate for $(n,\gamma)$. This test compares known $(n,\gamma)$

*rhatarik@lbl.gov; present address: Department of Chemistry, University of California, Berkeley, California 94720, USA.

 

cross sections with those deduced from $(d,p\gamma)$ reactions. Preliminary results have been reported previously [17–19].

In general the surrogate method is used to determine cross sections of reactions that are of the form $a + A \rightarrow B^* \rightarrow c + C$, that is, that go through a compound state $B^*$. Based on the assumption that formation $(a + A \rightarrow B^*)$ and decay $(B^* \rightarrow c + C)$ of the compound nucleus are independent of each other for each given spin and parity value, the desired cross section can be expressed as the product of the formation cross section and the decay probability [20,21]:

$$\sigma_{\alpha\chi}(E_x) = \sum_{J,\pi} \sigma_\alpha^{\mathrm{CN}}(E_x, J, \pi) P_\chi^{\mathrm{CN}}(E_x, J, \pi). \qquad (1)$$

Here $\sigma_{\alpha\chi}$ stands for the cross section for forming the compound nucleus via entrance channel $\alpha$ and its decay via exit channel $\chi$, $\sigma_\alpha^{\mathrm{CN}}$ is the formation cross section of the compound nucleus $(a + A)$ from the entrance channel $\alpha$ and $P_\chi^{\mathrm{CN}}$ is the decay probability into the exit channel $\chi$ $(c + C)$.

The formation cross section of the compound nucleus $(\sigma_\alpha^{\mathrm{CN}})$ can usually be determined from theory using optical model parameters, which can be calculated with relatively higher accuracy than the decay probability. In the present work, the reactions $n + {}^{171}\mathrm{Yb} \rightarrow {}^{172}\mathrm{Yb}^*$ and $n + {}^{173}\mathrm{Yb} \rightarrow {}^{174}\mathrm{Yb}^*$ for the entrance channel will be compared to the surrogate reactions $d + {}^{171}\mathrm{Yb} \rightarrow {}^{172}\mathrm{Yb}^* + p$ and $d + {}^{173}\mathrm{Yb} \rightarrow {}^{174}\mathrm{Yb}^* + p$, respectively.

In a surrogate measurement, the decay channel probabilities $P_\chi^{\mathrm{CN}}$ are measured and the compound-nucleus formation cross section is calculated to obtain the desired cross sections. In general, the decay probabilities depend on the spin and parity of the compound nucleus, but there are certain circumstances in which the decay probabilities depend only on the excitation energy of the nucleus, that is, the Weisskopf-Ewing (WE) limit [21]. In the WE limit, the sum over $J$ and $\pi$ in Eq. (1) is no longer necessary; most experimental surrogate measurements are based on the WE limit.

Assuming the validity of the WE limit in a $(d,p\gamma)$ measurement, the $\gamma$-ray decay probability of the compound nucleus is determined via

$$P_\gamma^{\mathrm{CN}}(E_x) = \frac{N_{(d,p\gamma)}(E_x)}{\epsilon N_{(d,p)}(E_x)}, \qquad (2)$$

where $N_{(d,p\gamma)}$ is the number of proton-$\gamma$ coincidences from reactions on the target, $N_{(d,p)}$ is the number of protons detected, and $\epsilon$ is the efficiency of detecting the $\gamma$ exit channel. One of the largest systematic uncertainties in Eq. (2) is $N_{(d,p)}$, owing mainly to background from $(d,p)$ reactions on target contaminants. In practice it is more reliable to measure ratios of cross sections. There are two forms of surrogate ratio methods (SRMs): an internal and an external SRM. The internal ratio method attempts to determine the cross-section ratio on two different exit channels of the same compound nucleus, whereas the external SRM uses the same exit channel on two different compound nuclei. The internal SRM was used in a benchmark experiment [15] to determine the neutron capture cross section of $^{235}\mathrm{U}$ relative to its fission cross section compared to the evaluation [22], whereas the present work benchmarks the external SRM for neutron capture on the $^{171}\mathrm{Yb}$ and $^{173}\mathrm{Yb}$ isotopes. The external SRM was also successfully applied in Refs. [7–10] and [14]. In an external SRM approach the cross-section ratio is determined by

$$\begin{aligned}\frac{\sigma_{n\gamma}^{(1)}(E_n)}{\sigma_{n\gamma}^{(2)}(E_n)} &= \frac{\sigma_n^{\mathrm{CN}(1)}(E_n) P_\gamma^{\mathrm{CN}(1)}(E_n)}{\sigma_n^{\mathrm{CN}(2)}(E_n) P_\gamma^{\mathrm{CN}(2)}(E_n)} \\ &= \frac{\sigma_n^{\mathrm{CN}(1)}(E_n) N_{(d,p\gamma)}^{(1)}(E_n) \epsilon^{(2)} N_{(d,p)}^{(2)}(E_n)}{\sigma_n^{\mathrm{CN}(2)}(E_n) N_{(d,p\gamma)}^{(2)}(E_n) \epsilon^{(1)} N_{(d,p)}^{(1)}(E_n)} \\ &\approx K \frac{N_{(d,p\gamma)}^{(1)}(E_n)}{N_{(d,p\gamma)}^{(2)}(E_n)}, \end{aligned} \qquad (3)$$

where the approximation is made that the ratios of the two neutron formation cross sections are identical and $N_{(d,p)}^{(1)}(E_n)/N_{(d,p)}^{(2)}(E_n)$ is independent of the equivalent neutron energy. The constant $K$ depends here on the formation cross sections of the compound nucleus in the $(d,p)$ reactions, the $\gamma$-cascade detection efficiency, the target thicknesses, and the integrated beam currents.

The goal of the present experiment was to test how well a $(d,p\gamma)$ surrogate reaction would reproduce known neutron capture cross sections. The neutron capture cross sections of the isotopes $^{171}\mathrm{Yb}$ and $^{173}\mathrm{Yb}$ are known up to neutron energies of 225 keV from the work of Wisshak *et al.* [23]. Because both isotopes are stable, direct kinematics was chosen because it allows better proton energy resolution and reduced Doppler broadening of the emitted $\gamma$ rays. The experiment was performed at the 88-Inch Cyclotron at Lawrence Berkeley National Laboratory. An 18.5-MeV deuteron beam was used to irradiate the two Yb targets. The data were taken over a period of 4 days, with the beam current varying between 2 and 3 enA (electrical nano Ampere). The two targets used were both self-supporting metallic foils of isotopically enriched ytterbium. The $^{171}\mathrm{Yb}$ target had an areal density of 981 $\mu\mathrm{g/cm}^2$; the $^{173}\mathrm{Yb}$ target, one of 502 $\mu\mathrm{g/cm}^2$. The outgoing reaction particles were detected with an array of annular segmented silicon detectors (Silicon Telescope Array for Reaction Studies; STARS [8,24]). The array consisted of three double-sided silicon detectors from Micron Semiconductor, which were located downstream of the target. The arrangement of the detectors consisted of a thin (500-$\mu$m; $\Delta E$) detector and two thick (1 000-$\mu$m; $E1$ and $E2$) stopping detectors, allowing for particle identification by examination of the energy loss in the $\Delta E$ detector relative to the total energy deposited (see Fig. 1). Forward angles from 44° to 77° were covered. Each detector is separated into rings in the front and wedge-shaped sectors on the back side, which allows the angle relative to the beam axis, as well as the azimuthal angle, to be determined. The determination of the angles from each detector separately can be used to trace the particle back to the target. Between the target and the silicon detectors was a 4.44 $\mathrm{mg/cm}^2$ aluminum foil to shield the detectors from $\delta$ electrons. The Livermore Berkeley Array for Collaborative Experiments, consisting of six compton suppressed HPGe clover detectors [25,26], was used to detect $\gamma$ radiation in coincidence with particles. The efficiency and energy calibrations of the germanium detectors were performed using a $^{152}\mathrm{Eu}$ source. The silicon detectors were calibrated using $\alpha$'s from a $^{226}\mathrm{Ra}$ source; each detector

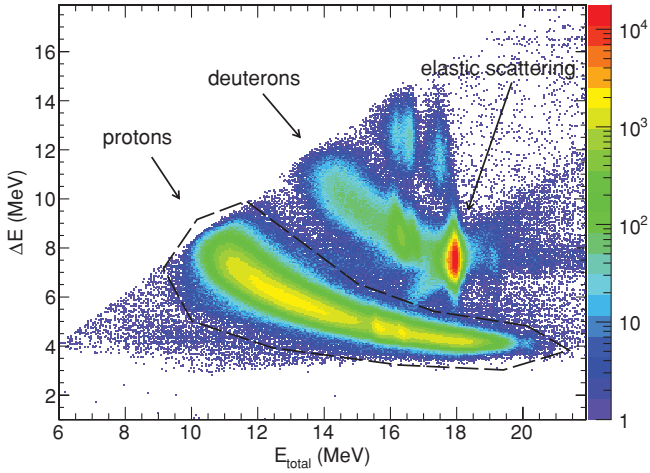


FIG. 1. (Color online) Energy deposited in the $\Delta E$ detector vs. the total energy $E$ of the particle in the center-of-mass frame. Protons and deuterons are clearly separated.

had an energy resolution of ≈70-keV FWHM (full-width half-maximum).

In a neutron-induced reaction, a compound nucleus with an excitation energy equal to the sum of the neutron separation energy and the kinetic energy of the neutron minus the energy of the recoil is formed. In the surrogate experiment the equivalent neutron energy is therefore given by subtracting the neutron separation energy from the excitation energy and applying a correction factor for the recoil energy in the neutron interaction case. To obtain the excitation energy of the compound nucleus for a given event, the proton energy was corrected for various energy losses (in the target, a $\delta$-electron shield and gold layers on the detectors). Then the energy of the recoil particle was calculated and the excitation energy of the compound nucleus was determined from the energy and angle of the outgoing proton (as described in Refs. [18] and [19]).

For each 60-keV-wide excitation energy bin a coincident $\gamma$-ray spectrum is obtained (see Fig. 2). To calculate the surrogate ratio, the proton-$\gamma$ coincidence rate for both targets

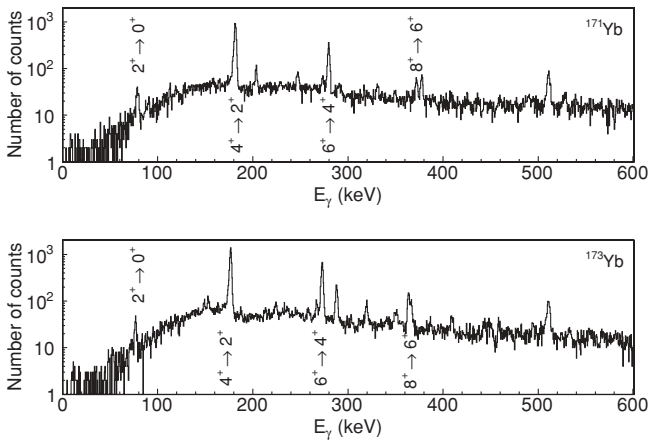


FIG. 2. $\gamma$-ray spectra for an excitation energy 30 keV above the neutron separation energy. The strongest transitions observed are from the ground-state band. Top, $^{171}$Yb; bottom, $^{173}$Yb target.

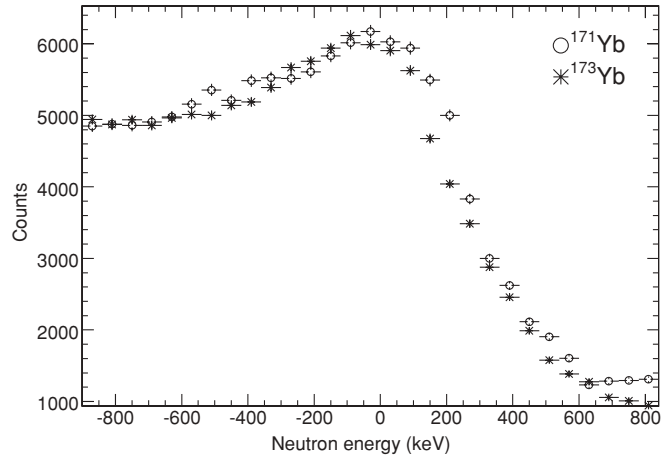


FIG. 3. Yield of the $4^+ \rightarrow 2^+$ transitions gated on protons as a function of the equivalent neutron energy for both targets.

has to be determined. Ideally a $\gamma$-ray line corresponding to a transition de-exciting a state that collects most of the de-excitation cascades of the compound nucleus should be used to "tag" the nucleus. Because both isotopes are even-even nuclei, the decay of the first excited $2^+$ state would be the preferred choice. However, this state is below 80 keV for both reaction products and the transition to the ground state has a low observed intensity owing to internal conversion and a lower detector efficiency. Therefore the $4^+ \rightarrow 2^+$ transition feeding the first excited $2^+$ state is the best candidate to collect the $\gamma$-decay cascade and deduce $N_{(d,p\gamma)}$ as a function of equivalent neutron energy in the compound nucleus.

The intensity of the $4^+ \rightarrow 2^+$ transition was determined for every equivalent neutron energy bin separately and is shown for both targets in Fig. 3. By using the intensities of the $4^+ \rightarrow 2^+$ transition as the yield for $N_{(d,p\gamma)}$, the efficiency $\epsilon$ in Eq. (2), will contain two parts: the detection efficiency of the germanium detector as well as the fraction of the $\gamma$ cascade that passes through the $4^+ \rightarrow 2^+$ transition. We assume that this fraction is, to first order, independent of excitation energy and part of the constant $K$ in Eq. (3). $K$ can be determined by evaluating this yield below the neutron separation energy. In this energy region $\gamma$ decay is the only possible mode of de-excitation, which implies that, for every proton observed, a $\gamma$-ray cascade is also emitted and the probability ratio is unity. This allows normalization of the yields of both targets below the neutron separation energy, where the normalization constant (which is $=1/K$) takes care of the different integrated beam current and target thicknesses. The surrogate cross-section ratio for these targets was determined by dividing the normalized count rate yields from the $^{171}$Yb target by those of the $^{173}$Yb target.

The ratios determined from the data in Fig. 3 disagree with the measured [23] ratio of $(n,\gamma)$ cross sections by 30%. Repeating the same procedure, integrating the $6^+ \rightarrow 4^+$ transitions measured in $(d,p\gamma)$, increases the difference to 50%. Because both transitions sample a different spin and parity distribution of the compound nucleus, this indicates a spin dependence of the decay probabilities, which implies that the WE limit does not apply. Although the limitations of the

WE assumption were not recognized in concurrent work, it is not surprising that the WE limit does not apply, as earlier work [24,27] suggests that this limit is applicable at higher excitation energies (>3 MeV) above the neutron separation energy. The neutron energy region of interest for $(n,\gamma)$ is in the kilo–electron volt region [23]. Therefore, in principle, the sum over all spins and parities given in Eq. (1) should be evaluated to deduce cross sections. Alternatively, conditions could be identified that favor a spin distribution similar to that produced by neutron capture. One problem in this analysis is that both targets had a different ground-state spin: $^{171}$Yb has $I^\pi = (1/2)^-$, whereas $^{173}$Yb has $I^\pi = (5/2)^-$.

Information about the spin of the compound nucleus produced in the reaction can be obtained either by using the angular distribution of the detected protons or by using the intensities of the $\gamma$-ray transitions as a function of spin. However, because the strongest contribution of the $(d,p)$ reaction is at forward angles, almost all of the experimental data are concentrated in the innermost rings. The variation of the results from gating on different ring groups was smaller than the statistical uncertainties of the data. Hence, the intensity of $\gamma$-ray transitions as a function of angular momentum were the only available insight into the spin distribution of the compound nucleus.

To model the expected intensities of $\gamma$-ray transitions, simulations of the $\gamma$-ray decay of the $^{172,174}$Yb compound systems were performed using the DICEBOX code [28]. In these simulations, the input consists of the experimental-level energies, their spins and decay modes for the discrete part of the nuclear excitation spectrum at lower excitation energies, and nuclear models for the level density and the photon strength functions at higher excitation energies. The statistical $\gamma$-ray cascade in the quasicontinuum regions is then simulated by the Monte Carlo technique.

Each simulation was done for an excitation energy of 100 keV above the neutron separation energy, with one simulation for each spin-parity combination from $J^\pi = 0^-$ to $J^\pi = 7^+$. The simulations that best reproduce the observed intensities of the $6^+ \rightarrow 4^+$ and $4^+ \rightarrow 2^+$ yrast transitions was for $J = 4$ for the $^{171}$Yb$(d,p\gamma)$ and $J = 5$ for the $^{173}$Yb$(d,p\gamma)$ reaction. This indicates that the average angular momentum transfer of the $(d,p\gamma)$ reaction is $\Delta\ell \approx 3$, whereas neutron capture in the kilo–electron volt region is mostly dominated by $s$-wave capture.

If one makes the simplified assumption that $(n,\gamma)$ is only $s$-wave capture, then $^{171}$Yb$(n,\gamma)$ would lead to a compound nucleus in a $0^-$ or $1^-$ configuration. The DICEBOX simulations for these spins and parities show that there should be almost no contribution to feeding of the $4^+$ yrast state from the $6^+$ state. A similar analysis can be made for the $^{173}$Yb$(d,p\gamma)$ and $^{173}$Yb$(n,\gamma)$ comparison. For the $^{173}$Yb target, the DICEBOX simulation indicates that the $6^+ \rightarrow 4^+$ transition should be about five times weaker following $s$-wave capture ($2^-$ or $3^-$ capture state) than what was experimentally observed for the $(d,p\gamma)$ reaction. This is an indication that the surrogate reaction populated higher spins than the neutron-induced reaction.

The DICEBOX results are summarized in Table I as the ratio of intensities for the yrast transitions $I(6^+ \rightarrow 4^+)/I(4^+ \rightarrow 2^+)$. This ratio also represents the fraction of feeding of the $4^+$ state from the $6^+$ state. Table I also summarizes the intensity ratios for these two yrast transitions in $^{172}$Yb and $^{174}$Yb following the $(d,p\gamma)$ reaction.

TABLE I. Intensity ratio $I(6^+ \rightarrow 4^+)/I(4^+ \rightarrow 2^+)$ from the present $(d,p\gamma)$ experiments compared to DICEBOX-simulated $s$-wave neutron capture.

| Target | $(d,p\gamma)$ experiment | DICEBOX simulation |
|---|---|---|
| $^{171}$Yb | $0.33 \pm 0.01$ | 0.02 |
| $^{173}$Yb | $0.54 \pm 0.01$ | 0.10 |

To select compound nuclei with a spin distribution closer to neutron capture, the feeding from the $6^+$ state was subtracted from the observed intensity of $4^+ \rightarrow 2^+$ transitions. This was done by subtracting the efficiency corrected area of the $6^+ \rightarrow 4^+$ line from the area of the $4^+ \rightarrow 2^+$ peak in the spectrum for each neutron energy bin separately; a comparison of the result obtained and the $(n,\gamma)$ cross-section ratio from Ref. [23] is shown in Fig. 4. The cross-section ratio is within 15% for $E_n > 90$ keV. Because the resolution for a particle detected by the silicon detector array was ≈100-keV FWHM, the lowest-energy bin contains significant contributions from below the neutron separation energy.

Demonstrating the effectiveness of the $(d,p\gamma)$ reaction as a surrogate for $(n,\gamma)$ is an important step toward deducing $(n,\gamma)$ cross sections on short-lived nuclei. However, significant

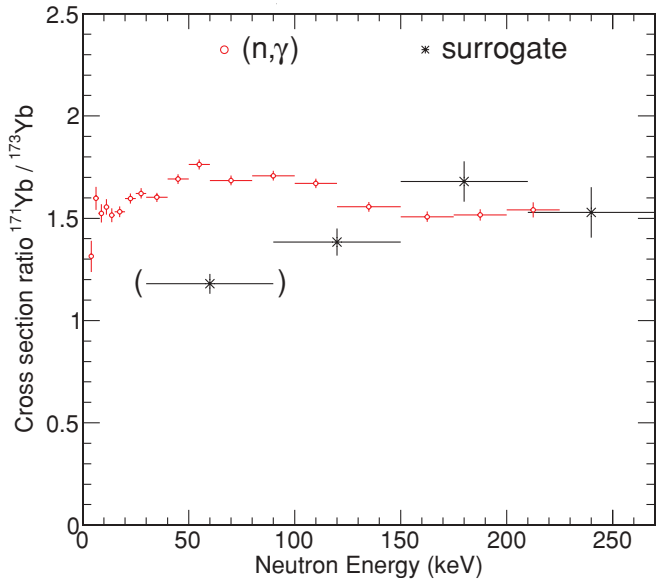


FIG. 4. (Color online) Comparison of cross-section ratio results between the measured $(n,\gamma)$ values from Ref. [23] and those deduced from the present $(d,p\gamma)$ measurements using the $4^+ \rightarrow 2^+$ transition intensity with feeding via the $6^+ \rightarrow 4^+$ transition subtracted. The cross-section uncertainties shown are only statistical errors. The lowest data point is in parentheses, as it contains significant contributions from below the neutron separation energy owing to detector resolution.

challenges remain. The experiment described served as a benchmark to test the feasibility of measuring a $(d,p\gamma)$ surrogate in inverse kinematics. These techniques are being developed at the Holifield Radioactive Ion Beam Facility (HRIBF) at Oak Ridge National Laboratory (ORNL), building on the initial efforts in Ref. [16]. The bins for effective neutron energy will be large (>200 keV) because of the energy loss of beams traversing targets of finite thickness (>100 $\mu$g/cm$^2$). Reaction protons need to be measured in coincidence with beamlike recoils to minimize background protons from fusion with the carbon in the $CD_2$ targets. And a highly efficient $\gamma$-ray detector array, with the ability to correct for Doppler effects, is required. Current efforts [29] at the HRIBF at ORNL are focused on addressing the technical challenges using the newly commissioned ORRUBA array of position-sensitive silicon strip detectors for reaction protons [30]. Next steps include furthering the validation of the $(d,p\gamma)$ reaction as a surrogate for $(n,\gamma)$ on unstable nuclei by inverse kinematics $(d,p\gamma)$ measurements with beams of stable nuclei for which $(n,\gamma)$ cross sections have been measured.

To summarize, we have demonstrated that decay probabilities from the $^{171,173}$Yb$(d,p\gamma)$ reaction stay within 15% of the measured [23] ratio of $^{171,173}$Yb$(n,\gamma)$ cross sections for effective neutron energies $E_n > 90$ keV. Because of the low energies above the neutron separation energy that characterize neutron capture, not surprisingly, the WE limit is not valid. However, by selecting $\gamma$-ray transitions in the surrogate reaction that mimic those strongly populated in $(n,\gamma)$, informed by a statistical model such as DICEBOX calculations [28], the spin dependence of the decay of compound-nuclear states can be compensated for in the surrogate analysis.

The authors thank the operations staff of the 88-Inch Cyclotron and M. Krtička for advice on DICEBOX calculations. This work was supported in part by the US Department of Energy under Contract Nos. DE-FG52-03NA00143 (Rutgers University), DE-AC52-07NA27344 (Lawrence Livermore National Laboratory), and DE-AC02-05CH11231 (Lawrence Berkeley National Laboratory) and the US National Science Foundation.

[1] J. Beun *et al.*, J. Phys. G **36**, 025201 (2009).
[2] R. Surman, J. Beun, G. C. McLaughlin, and W. R. Hix, Phys. Rev. C **79**, 045809 (2009).
[3] Nuclear Science Advisory Committee, Report to NSAC of the Subcommittee on Isotopes for the Nation's Future: A Long Range Plan (2009).
[4] L. Schroeder and E. Lusk, presented at the Nuclear Physics and Related Computational Science R&D for Advanced Fuel Cycles workshop, Bethesda, MD, 2006.
[5] W. Hauser and H. Feshbach, Phys. Rev. **87**, 366 (1952).
[6] J. D. Cramer and H. C. Britt, Nucl. Sci. Eng. **41**, 177 (1970).
[7] C. Plettner *et al.*, Phys. Rev. C **71**, 051602(R) (2005).
[8] J. T. Harke *et al.*, Phys. Rev. C **73**, 054604 (2006).
[9] B. F. Lyles *et al.*, Phys. Rev. C **76**, 014606 (2007).
[10] S. R. Lesher *et al.*, Phys. Rev. C **79**, 044609 (2009).
[11] W. Younes and H. C. Britt, Phys. Rev. C **68**, 034610 (2003).
[12] M. Petit *et al.*, Nucl. Phys. **A735**, 345 (2004).
[13] S. Boyer *et al.*, Nucl. Phys. **A775**, 175 (2006).
[14] B. L. Goldblum *et al.*, Phys. Rev. C **78**, 064606 (2008).
[15] J. M. Allmond *et al.*, Phys. Rev. C **79**, 054610 (2009).
[16] J. A. Cizewski *et al.*, Nucl. Instrum. Methods B **261**, 938 (2007).
[17] R. Hatarik *et al.*, AIP Conf. Proc. **1005**, 105 (2008).
[18] R. Hatarik *et al.*, AIP Conf. Proc. **1099**, 812 (2009).
[19] R. Hatarik *et al.*, AIP Conf. Proc. **1090**, 445 (2009).
[20] J. Escher *et al.*, J. Phys. G **31**, S1687 (2005).
[21] J. E. Escher and F. S. Dietrich, Phys. Rev. C **74**, 054601 (2006).
[22] M. B. Chadwick *et al.*, Nucl. Data Sheets **107**, 2931 (2006).
[23] K. Wisshak, F. Voss, C. Arlandini, F. Käppeler, and L. Kazakov, Phys. Rev. C **61**, 065801 (2000).
[24] L. A. Bernstein *et al.*, AIP Conf. Proc. **769**, 890 (2005).
[25] G. Duchêne, Nucl. Instrum. Methods A **432**, 90 (1999).
[26] Z. Elekes *et al.*, Nucl. Instrum. Methods A **503**, 580 (2003).
[27] C. Forssén, F. S. Dietrich, J. Escher, R. D. Hoffman, and K. Kelley, Phys. Rev. C **75**, 055807 (2007).
[28] F. Becvár, Nucl. Instrum. Methods A **417**, 434 (1998).
[29] W. A. Peters *et al.*, Bull. Am. Phys. Soc. **53** (12), 95 (2008).
[30] S. D. Pain *et al.*, Nucl. Instrum. Methods B **261**, 1122 (2007).